Characterizing centrosymmetric two-ring PAHs using jet-cooled high resolution mid-infrared laser spectroscopy and anharmonic quantum chemical calculations

S Chawananon, O Pirali, M Goubet, P Asselin

Characterizing centrosymmetric two-ring PAHs using jet-cooled high resolution mid-infrared laser spectroscopy and anharmonic quantum chemical calculations

S. Chawananon[a], O. Pirali[b,c], M. Goubet[d] and P. Asselin[a,*]

[a]*Sorbonne Université, CNRS, MONARIS, UMR 8233, 4 place Jussieu, Paris, F-75005 France.*
[b]*AILES Beamline, Synchrotron SOLEIL, l'Orme des Merisiers, Saint-Aubin, 91192 Gif-sur-Yvette cedex, France.**
[c]*Université Paris-Saclay, CNRS, Institut des Sciences Moléculaires d'Orsay, 91405 Orsay, France.*
[d] *Univ. Lille, CNRS, UMR 8523 - PhLAM - Physique des Lasers Atomes et Molécules, F-59000 Lille, France.*

Abstract

The presence of Polycyclic Aromatic Hydrocarbons (PAH) molecules in the interstellar medium, recently confirmed by the detection of cyano-naphthalenes, renews the interest of extensive spectroscopic and physical-chemistry studies about such large species. The present study reports the jet-cooled rovibrational IR study of three centrosymmetric two-ring PAH molecules, naphthalene ($C_{10}H_8$), [1,5] naphthyridine ($C_8H_6N_2$) and biphenyl ($C_{12}H_{10}$) in the in-plane ring C-H bending (975-1035 cm^{-1}) and C-C ring stretching (1580-1620 cm^{-1}) regions. For the two most rigid PAHs, the accuracy of spectroscopic parameters derived in ground and several excited states (6 for naphthalene and 6 for [1,5] naphthyridine) has significantly improved the literature values. In addition, comparison between experiments and quantum chemical calculations confirms the predictive power of the corrected calculated rotational parameters. The more flexible structure of biphenyl makes particularly challenging the analysis of high resolution jet-cooled spectra of ν_{19} and ν_{23} modes recorded at about 1601 and 1013 cm^{-1} respectively. The presence of three torsional vibrations below 120 cm^{-1} together with small values of the rotational constants prevented us to determine the ground and ν_{19}=1 excited rotational constants independently. In the ν_{23} band region, the presence of two bands rotationally resolved and separated by only 0.8 cm^{-1}, raises the question of possible splittings due to a large amplitude motion, most probably the torsion of the aliphatic bond between the two phenyl rings.

I. Introduction

Polycyclic Aromatic Hydrocarbons (PAH) molecules, together with their numerous derivatives, in particular nitrogen containing species (PANHs), have long been proposed as carriers of the so-called Aromatic Infrared bands (AIBs) observed in a large variety of astrophysical objects between 3 and 20 µm.[1,2] These species are particularly important for the physical-chemistry processes occurring in space as numerous laboratory experiments and theoretical studies have shown that PAHs could be the fundamental bricks in the condensation process of soot particles.[3] Very recently, the detections of benzonitrile[4], cyano-naphthalenes[5] and indene[6] in TMC-1 provided the first unambiguous confirmations of the interstellar PAHs hypothesis and raised new questions concerning the formation and destruction pathways of such systems in interstellar environments.

* Corresponding author : pierre.asselin@upmc.fr

In the infrared (IR) domain, the constant improvement of both spectral resolution and sensitivity of observational instruments made it possible to extract valuable information from AIBs profiles, in particular about the dependence of the vibrational modes on molecular properties such as size distribution, ionization states, protonation, nitrogen substitution and contribution from nanometric grains.[7] In this context, the recent launch of the James Webb Space Telescope (JWST) will open exciting perspectives for which new laboratory measurements performed at high spectral resolution may be of high interest to the exploitation of future astronomical observations.

In the laboratory, high-resolution (HR) sensitive experiments enabled the measurement rotationally resolved spectra of relatively small PAH compounds in the micro-wave (MW) and millimeter-wave (mmW), in the infrared (IR) and in the ultraviolet-visible (UV-vis) spectral ranges. For species possessing a permanent electric dipole moment, jet-cooled HR Fabry-Perot Fourier Transform MW (FP-FTMW) [8-11] provided accurate ground state (GS) rotational parameters for several two-ring and few three-ring species which were exploited as reference data to test the accuracy of anharmonic calculations.[12]

Regarding centrosymmetric PAHs, the absence of permanent dipole moment prevents the use of MW techniques to study the rotational structure of these species in their GS. In such cases, high resolution spectroscopy in the IR and UV-vis spectral ranges give access to ground state rotational parameters from analyses of rovibrational and rovibronic transitions. However, HR IR studies of rotationally resolved vibrational bands of large C-bearing molecules are still very scarce. Albert *et al.*[13] recorded the far-IR spectra of naphthalene and indole in the 600-900 cm^{-1} range using a synchrotron-based Fourier transform spectrometer (FTS) coupled to a long path absorption cell at room temperature (RT). Due to the congested rotational structures and the presence of many hot bands[14-16], the spectral analysis remained challenging and highlights the need to probe such large molecular systems at low temperatures[17], and using sensitive HR IR spectrometers. Brumfield *et al.*[18] developed a sensitive set-up combining cavity ring down spectroscopy (CRDS) in a continuous supersonic jet expansion, enabling them to record and analyze a C-H bending mode of pyrene relatively narrow spectral regions. Alternatively, at the synchrotron facility SOLEIL, some of the authors of the present paper exploited both a RT long absorption cell and a continuous supersonic jet (Jet-AILES) coupled to an FT spectrometer to resolve the rotational structure of three far-IR bands of naphthalene[19]. However, the Jet-AILES set-up[20] remains limited in sensitivity for two following main reasons. (i) The acquisition mode of a scanning FTS imposes its coupling with continuous gas flows. In these conditions, the acquisition of high-resolution spectra required the consumption of several kg of solid sample, which strongly limits the investigation of PAHs other than naphthalene.[19] (ii) Because of the high residual pressure in the expansion chamber, the implementation of a multipass optical system probing only cold samples is very challenging. Alternatively to supersonic experiments, a powerful approach has been recently implemented by Changala *et al.*[21,22] who integrated a cavity-enhanced-direct frequency comb spectroscopy (CE-DFCS) technique with buffer gas cooling experiment. Spectra of several large organic molecules such as naphthalene and C_{60} were recorded in the mid-IR range, under cold and thermally equilibrated conditions. Finally, in the UV-vis range, jet-cooled sub-Doppler excitation spectroscopy of the $\widetilde{A}^1B_{1u} \leftarrow \widetilde{X}^1A_g$ electronic transition of naphthalene provided reliable GS constants thanks to wavenumber accuracies and experimental linewidths comparable to IR experiments.[23,24]

In the present work, a tunable mid-IR quantum cascade laser (QCL) spectrometer coupled to a pulsed supersonic jet (SPIRALES set-up) has been recently implemented within the MONARIS laboratory to record rotationally resolved spectra of molecular complexes and large molecules at low rovibrational temperatures. Recent studies obtained with SPIRALES emphasized its ability to extract structural information about low volatile heavy polyatomic molecules.[25,26] The spectrometer is equipped with three tunable QCLs working in the mid-IR range around 6 and 10 µm, enabling us to probe several characteristic fundamental vibrations of PAH molecules.

As a support to rotational analyses, predictive quantum chemistry calculations are invaluable, in particular when dealing with congested spectra. Using commercially available programs such as Gaussian, calculations at the anharmonic level are required since the rotational constants of vibrationally excited states are obtained from the second order vibrational perturbation theory (VPT2). Although the use of density functional theory (DFT) has shown some encouraging results[27], high level *ab initio* calculations are still preferred[28] but those techniques applied to anharmonic calculations are very time consuming in the case of large molecules. Accurate determination of the molecular structure is essential to predict the rotational fingerprints but requires the determination of vibrational corrections to rotational constants and at least the quartic centrifugal distortion constants, implying the computation of cubic force fields and the corresponding VPT2 analysis.[29,30]

The present study is dedicated to the rovibrational study of three centrosymmetric bicyclic PAHs, naphthalene ($C_{10}H_8$), [1,5] naphthyridine ($C_8H_6N_2$) and biphenyl ($C_{12}H_{10}$). Jet-cooled QCL experiments were guided by low-resolution FTS data and anharmonic calculations. For each species, two vibrational modes were targeted in the available QCL spectral ranges: ν_{35} and ν_{19} for naphthalene, ν_{32} and ν_{39} for [1,5] naphthyridine and ν_{23} and ν_{19} for biphenyl. In previous studies, three far-IR c-type bands of naphthalene (ν_{46} in jet and cell, ν_{47} and ν_{48} in cell) and two far-IR c-type bands of [1,5] naphthyridine (ν_{22} and ν_{18} in cell) were already analyzed, leading to a relatively accurate set of GS constants.[19,31] For these two PAHs, the purpose of the present study is to improve the accuracy of GS rotational parameters with respect to existing data by recording rovibrational jet-cooled spectra of bands exhibiting different selection rules than only the c-type bands analyzed in the literature. Due to its conformational peculiarities in crystalline, liquid and gas phases, biphenyl is a flexible hydrocarbon for which vibrational modes were only recently investigated using low resolution FTS in the gas phase.[32] Our objective is to investigate the spectral ranges covered by our QCLs to obtain the first HR data and derive reliable sets of rotational constants. Experimental rotational constants of these two-ring PAHs are then compared to anharmonic DFT calculations for modes involving higher energy vibrations to evaluate the predictive power of our approach. Last, GS experimental inertial defects for naphthalene and [1,5] naphthyridine complemented by other polycyclic aromatic molecules are used to adjust semi-empirical relations to estimate the zero-point inertial defect of aromatic compounds accounting for the contribution of lowest frequency out-of-plane (oop) modes.

II. Methods

A. QCL infrared spectroscopy experiment

The rovibrational spectra of naphthalene, [1,5] naphthyridine and biphenyl have been recorded in two specific spectral regions of PAH absorptions: the C-H in-plane bending and the C-C ring stretching vibrations. Infrared direct absorption experiments were performed with the SPIRALES set-up, a jet-cooled laser spectrometer which couples an external-cavity quantum cascade laser (EC-QCL) and a pulsed supersonic free jet to probe gas phase molecules cooled in the adiabatic expansion. SPIRALES has already been described in detail in recent papers[25,33] and only the main characteristics and most recent developments are presented hereafter.

The IR source is a continuous-wave room-temperature mode-hop-free EC-QCL (Daylight Solutions) of 10 MHz spectral width. The QCL chip and a diffraction grating are mounted on a piezoelectric transducer (PT) to form an external cavity, and high resolution measurements are obtained by scanning the length of this cavity. In the present study, two EC-QCLs were used to cover the following spectral ranges: 975–1035 cm^{-1} (Model 41103-MHF) and 1580-1620 cm^{-1} (Model

41062-MHF). About 8 % of the total power is used by an etalon consisting of a 0.025 cm^{-1} free-spectral-range confocal Fabry–Perot cavity, to provide a relative frequency scale. Absolute frequency calibration is obtained by passing about 8 % of the IR total radiation through a 10 cm length cell containing a known reference gas. A linear interpolation of the positions of the etalon maxima establishes the relationship between the voltage applied to the PT and the relative frequency. This new frequency scale enables to correct the free spectral range value of the reference fixed at the beginning of each experiment. A typical frequency accuracy of about 0.0005 cm^{-1} is achieved by comparing the frequency deviation of our measured lines of methanol (in the 975–1035 cm^{-1} range) NH_3 and H_2O (in the 1580–1620 cm^{-1} range) with frequency standards from the HITRAN2016[34] database. About 85% of the initial laser power is directed toward a multipass absorption cavity, based on an astigmatic variant of the off-axis resonator Herriott configuration. This optical cavity composed of two 1.5 inch astigmatic mirrors (R = 99.2%, AMAC-36, Aerodyne Research) is installed in the supersonic expansion chamber, perpendicularly to the jet axis. With respect to the square spot pattern of the initial optical configuration adjusted for 182 passes, the present optical settings were modified to obtain a rectangular spot pattern overlapping better with the planar expansion but with about half of the optimum number of optical passes.

The molecular jet was produced from a pulsed 0.9 mm diameter pin hole nozzle from General Valve Series 9 controlled by a valve driver (Iota One, Parker Hannifin). PAH compounds were seeded in the supersonic jet using a brass block fitted to a Dural reservoir filled with 1 g of solid sample. The reservoir located upstream, nearby the expansion zone, was heated up to 420 K to increase the sample vapor pressure which was carried by the argon flow. Typical dilution conditions used in this work were about 1 % of PAH in 2 bar of Ar. The seeded mixture was then cooled down by converting the circular flow of the standard valve configuration into a planar expansion using six-way distribution gas channel capped with two modified industrial blades[35], forming a 30 mm length and 150 µm width slit aperture. Jet-cooled PAH molecules were probed over axial distances between 5 and 15 mm from the nozzle exit due to the relatively large zone covered by the different trajectories of the IR beam in the multipass optical system.

Jet-cooled spectra were recorded using a rapid scan scheme similar to set-ups developed previously and described in Ref [36]. The QCL frequency is scanned by a sine wave with an amplitude of up to 80 V to the PT at frequencies up to 100 Hz, which corresponds to a sweep of 0.8 cm^{-1} in 5 ms with a frequency sampling of about 3 MHz. A baseline-free transmittance through the multipass cavity is obtained by taking the ratio of signals recorded in the presence and absence of the jet.

B. Fourier Transform Spectroscopy (FTS) experiment

Along with SPIRALES experiments, we exploit here a series of broadband mid-IR spectra (500-3500 cm^{-1}) of the three PAH molecules under study, previously recorded using the FT interferometer Bruker IFS 125 located at the AILES beamline of the SOLEIL synchrotron facility. The FT spectrometer was equipped with a Globar source, a KBr beamsplitter and a liquid N_2 cooled HgCdTe detector. The maximum vapor pressure at room temperature of each compound was injected in a 150 m absorption RT path cell (White-type arrangement) equipped with ZnSe windows. The three PAH spectra shown in Figure 1 result of the Fourier transform of 1000 coadded interferograms at 0.5 cm^{-1} spectral resolution. Low resolution FT spectra of [1,5] naphthyridine and biphenyl had been already published in Refs [31] and [32], respectively. The same set-up has been used to record the high resolution spectra of the ν_{24} band of naphthalene and the ν_{42} band of [1,5] naphthyridine. The acquisition of these far-IR absorption spectra at ultimate resolution (0.001 cm^{-1}) required using the far-IR synchrotron radiation continuum, 50 μm thick polypropylene windows, a 6 μm composite mylar beamsplitter, and a liquid He cooled Si bolometer detector.

C. Quantum chemical calculations

Previous studies on naphthalene and [1,5] naphthyridine enabled us to use experimental GS and ES rotational constants to calibrate quantum chemical calculations.[19,31] Thanks to the good agreement obtained between experimental data and anharmonic DFT calculations, the present study exploits the results of quantum chemical calculations already published.[19,31] These calculations were conducted using the Gaussian 09 rev C.01 software package[37] and based on optimized equilibrium structures and vibrational frequencies calculated using the B97-1 density functional with the ANO-RCC basis set reduced to a double-ζ polarization level (ANO-DZP).[38] The use of a too small basis set led to overestimates of bands origins and the best compromise to calculate reliable anharmonic frequencies and obtain good estimates of rotational constants comes from the B97-1/cc-pVTZ combination.[39] The good agreement obviously comes from error compensations between DFT methods that tend to optimize too loose geometries and an overestimation of the basis set superposition error.[40]

In the present study, new anharmonic calculations of biphenyl molecule have been performed at the same level as naphthalene and [1,5] naphthyridine with the dihedral angle θ between two phenylic groups predicted around 39°. Fig.2 displays the optimized structure of the three PAHs.

.

III. Analyses and results

As mentioned in the introduction, naphthalene and [1,5] naphthyridine have already been investigated using high resolution spectroscopy techniques[19,31]. The existing sets of GS parameters have been obtained from the combined analysis of out of plane vibrations (c-type bands) located in the far-IR range. Accessing to the characteristic in plane C-H bending and C-C stretching vibrations of these aromatics with our mid-IR laser spectrometer gives us the possibility to observe a-type and b-type bands with different selection rules regarding ΔK_a and ΔK_c. As a consequence, combined fits including various types of rovibrational transitions allowed us to retrieve a more reliable set of GS rotational constants. All data were fitted using a Watson type semi-rigid model for asymmetric tops[41] (A reduction in the I^r representation) developed up to the quartic centrifugal distortion (CD) terms using the PGOPHER[42] and the SPFIT/SPCAT programs.[43] Line assignments, measured frequencies, experimental uncertainties and deviations from the final global fits for naphthalene and [1,5] naphthyridine will be published in open access databases devoted to spectroscopic laboratory measurements.

A. Naphthalene

Naphthalene is an asymmetric top rotor close to the prolate limit (Ray's parameter κ = -0.68) belonging to the D_{2h} point group, with 48 vibrational modes of which 36 (with the symmetries b_{1u}, b_{2u} and b_{3u}) are infrared active. Two mid-IR bands, the in-plane C-H ring bending (ν_{35}) and the C-C ring stretching (ν_{19}) modes have been observed with the SPIRALES set-up. The presence of a Q-branch for the ν_{35} band, (located at 1012.011 cm^{-1}, see Fig.3a) and its absence in the band contour of the ν_{19} band (Fig. 4a) agree well with calculations indicating that these bands are a-type and b-type, respectively. Both bands were first analyzed using the v_{19}=1 and v_{35}=1 rotational constants from anharmonic B97-1/cc-pVTZ//ANO-DZP predictions scaled by the experimental values from Ref.[19]. In addition to the jet-cooled data, we undertook the analysis of the weak far-IR bands ν_{24} (b-type band around 359 cm^{-1}, 1.6 km/mol) and ν_{36} (a-type band around 620 cm^{-1}, 3.4 km/mol) previously recorded using the synchrotron-based RT set-up.[19] The absence of a Q-branch in the ν_{36} band contour suggests a strong perturbation of its rotational structure, probably involving the (ν_{47} + ν_{48}) combination band located about 20 cm^{-1} at higher frequency. On the other hand, the weaker ν_{24} band could be successfully analyzed. 1596 transitions involving J'< 100 and K_a < 100 were used to fit the ν_{24} parameters to the experimental accuracy of 0.0003 cm^{-1}. The combined fit CF-6 of naphthalene (including the vibrational states GS, v_{46}=1, v_{47}=1, v_{48}=1, v_{24}=1, v_{35}=1, v_{19}=1) was performed. Band centers, rotational and quartic CD constants (except for δ_J and δ_K) were fitted for the v_{46}=1, v_{47}=1,v_{48}=1 and v_{24}=1 vibrational states observed in the RT cell, and only band centers together with the rotational constants for the v_{35}=1 and v_{19}=1 vibrational states observed in the jet experiment. A total of 24215 lines including 3 c-type, 2 b-type, and one a-type bands were fitted to instrumental accuracy with a Root Mean Square (RMS) value of 0.0004 cm^{-1}. The new GS and 6 upper states rotational parameters are reported in Table 1.

Figs.3b and 4b display a comparison between the SPIRALES experimental spectra of both ν_{35} and ν_{19} modes of naphthalene and a PGOPHER simulation based on adjusted molecular parameters of CF-6 (Table 1) with a rotational temperature of 25 K and a full-width at half maximum (FWHM) of the rotational transitions of 0.0015 cm^{-1} for the ν_{35} band and 0.002 cm^{-1} for the ν_{19} band, which nearly follows the linear frequency dependence of the Doppler broadening.

B. [1,5] Naphthyridine

Like naphthalene, [1,5] naphthyridine is a nearly prolate asymmetric top (κ = -0.66) belonging to the C_{2h} point group with 42 vibrational modes of which 21 are infrared active. Using the synchrotron-based FTS experiment, Gruet *et al*.[31] performed the combined study of two intense c-type far-IR bands (ν_{22} and ν_{18} modes centered at about 166 and 818 cm^{-1}, respectively), to derive GS and ES constants. However, line congestion observed at high values of J and K_a originating from the combination of hot band structures together with the large rotational distribution prevented the authors to follow series with different K_a values. In the present study, the jet-cooled spectra of ν_{39} (Fig. 5a) and ν_{32} (Fig. 6a) fundamental modes were observed at about 1017 cm^{-1} (2.7 km/mol) and 1599 cm^{-1} (17.5 km/mol), respectively, as predicted by anharmonic calculations and observed at low resolution in Ref. [31]. An unexpected band detected around 1604 cm^{-1} (Fig. 7a), about ten times weaker than the ν_{32} band, emphasizes the high sensitivity of the SPIRALES set-up. The definitive assignment of this band is uncertain but among the different possibilities of combination bands calculated in this spectral range with harmonic intensities around 1 km/mol, the most probable candidate is the (ν_{23} + ν_{19}) combination band calculated at 1602 cm^{-1}. Starting from the set of GS rotational constants of Gruet *et al.*[31], the three bands were analyzed separately. In addition to the QCL results, we studied the room temperature absorption spectrum of the weak ν_{42} band (392 cm^{-1}, 8.7 km/mol) previously observed in the synchrotron-based RT experiment.[31] The combined fit CF-6 of [1,5] naphthyridine (including the vibrational states GS, v_{22}=1, v_{18}=1,v_{42}=1, v_{39}=1, v_{32}=1, v_{23},v_{19}=1,1) was performed. In CF-6, GS quartic CD constants are kept fixed to the calculated values, while for the ES observed in the RT cell (v_{22}=1, v_{18}=1,v_{42}=1) all quartic CD constants are adjusted (except for δ_J and δ_K) and for the excited observed in jet (v_{39}=1, v_{32}=1, v_{23},v_{19}=1) all quartic CD constants are fixed to GS values. A total of 6445 lines involving 2 c-type and 4 a-type bands were fitted with a RMS value of 0.0003 cm^{-1}. The new GS and 6 ES rotational parameters are reported in Table 2. The simulated spectra of ν_{39}, ν_{32} and (ν_{23} + ν_{19}) bands of [1,5] naphthyridine together with the experimental ones are shown on Figs 5b, 6b, 7b, respectively.

C. Biphenyl

Due to the possible large amplitude motion around the single bond between the two phenyl rings, the conformational structure of biphenyl changes depending on the phase: the molecule is planar under normal conditions of temperature and pressure in the crystalline state but is twisted in the liquid and gas phases. Its structure has been extensively studied using a large panel of gas phase spectroscopic methods (electron diffraction, electronic excitation, absorption) from far-IR to UV ranges,[44-46] from which the dihedral angle θ between the two rings was determined experimentally (θ= 45 ± 10°) while its theoretical value lies in the 40-43° range.[47]

In the gas phase, biphenyl is an asymmetric top very close to a prolate rotor (κ = -0.97), resulting in a tighter substructure in K_a,K_c. than naphthalene and [1,5] naphthyridine. In its lowest-energy conformation, biphenyl belongs to the D_2 point group. Its axial orientation shown in Fig. 2 corresponds to minimum moment of inertia for the *z* axis and maximum moment of inertia for the *x* axis. Biphenyl has 60 vibrational modes of which 45 (having the B_1, B_2 and B_3 symmetries) are infrared active. FTIR absorption spectra of biphenyl were taken by Martin-Drumel *et al.*[32]. The comparison of the experimental spectrum with harmonic and anharmonic calculations allowed the assignment of 18 vibrational modes with a MAE of 0.77% for the B97-1/6-311G(d,p) method which appeared to be the best compromise to predict vibrational frequencies in terms of accuracy and computational cost.[32]

The HR infrared study of biphenyl turned out to be particularly challenging for the following reasons: (i) the smaller rotational constants of biphenyl (about 500 MHz for *B* and *C* compared to 1200 and 900 MHz for naphthalene and [1,5] naphthyridine, respectively) increase the spectral congestion; (ii) its non-rigidity gives rise to very low lying torsional vibrations (*i.e.* the ν_{15}, ν_{60} and ν_{44} modes of biphenyl located at 60, 92 and 118 cm^{-1}, respectively)[32] compared to naphthalene and [1,5] naphthyridine for which the lowest modes are around 160 cm^{-1}, so that the presence of relatively intense hot bands is expected even under jet-cooled conditions; (iii) the larger number of vibrational modes (30% higher with respect to the two other PAHs) combined with numerous low frequency modes lead to a much larger density of vibrational states which probably increases the number of possible anharmonic perturbations and intramolecular vibrational redistribution (IVR); (iv) it is difficult to anticipate the non-rigidity of the aliphatic bond torsion motion for vibrational energies above 1000 cm^{-1} but the occurrence of splittings due to internal rotation cannot be excluded; (v) last, due to the possible presence of large amplitude motions in biphenyl, anharmonic B97-1/cc-pVTZ//ANO-DZP methods successfully used to calculate rotational parameters of rigid PAHs are expected to be less predictive in the perspective of a HR rovibrational analysis.

Using the the low-resolution FTIR spectrum (Fig. 1) of biphenyl two modes were targeted with our SPIRALES set-up: the ν_{19} and ν_{23} modes located at about 1601 and 1013 cm^{-1} with harmonic intensities calculated at 12 and 7 km/mol, respectively. The ν_{19} band spectrum displayed a characteristic a-type band contour (Fig.8a) with a Q branch centered at 1604.87 cm^{-1} and, as expected, many broad unresolved features distributed over 0.2 cm^{-1} on both sides of the Q branch. Compared to rigid PAHs, we note that the accuracy of biphenyl analyses is degraded due to: (i) the stacking of up to ten ^QP and ^QR transitions within few thousandths of cm^{-1} in the P and R branches, which does not enable us to resolve the K_a,K_c substructure (ii) the presence of several low lying vibrational levels sufficiently populated in the planar expansion provides significant absorptions blurring of the fundamental band, particularly between the intense ^QP and ^QR lines. The main hot band contribution originates from the lowest frequency mode ν_{15}, calculated at 60 cm^{-1}. This hot band is probably responsible from the asymmetry of the Q branch on the low frequency side where three submaxima separated by 0.008 cm^{-1} are observed, tentatively assigned to $n\nu_{15} + \nu_{19} \leftarrow n\nu_{15}$ transitions up to n=3.

These transitions represent the main hot band contribution, estimated to about 10-15% of the total intensity of the cold fundamental band for a vibrational temperature around 40 K. Other hot band Q branches located at about 1604.68, 1604.70 and 1605.01 cm^{-1} are observed in the spectrum, probably involving higher low frequency modes as well as combination bands. However, their assignment remains uncertain because it would require extremely accurate calculations of the anharmonicity matrix. The variations of the rotational constants of the anharmonic B97-1/cc-pVTZ//ANO-DZP predictions are used as initial guess for the spectral analysis of the ν_{19} band and our best agreement is obtained for a rotational temperature of 25(5) K (Fig.8b). Due to line stacking and hot band structures, the GS *A* constant had to be fixed to its calculated value while GS *B* and *C* and the three ES rotational constants of the v_{19}=1 state are adjusted. The consequences of line stacking on the quality of our simulation are visible in Fig.8b: the sets of GS and v_{19} = 1 molecular parameters obtained do not reproduce the small frequency differences of the ^{Q}R transitions, leading to a less intense R branch, while the line stacking of the ^{Q}P transitions with quasi-equal frequencies is responsible from an intense P branch.

Two HR spectra recorded in the ν_{23} band region of biphenyl are shown in Fig.9a: a RT long path cell FT spectrum recorded at 0.005 cm^{-1} resolution displaying a characteristic PQR band contour centered around 1013 cm^{-1} and spread out over 20 cm^{-1}, and a SPIRALES jet-cooled spectrum showing two resolved *Q*- branches very close in frequency at 1012.8 and 1013.6 cm^{-1}. From the comparison between frequency positions of jet-cooled and RT Q branches (Fig. 9a), the jet-cooled *Q*-branch at 1013.6 cm^{-1} correlates well with the onset of the RT *Q*- branch which could correspond to the fundamental ν_{23} band. The assignment of the second band at 1012.8 cm^{-1} raises some questions: the possibility of a combination band close to this frequency with harmonic intensity larger than 1 km/mol has been examined from DFT calculations but no convincing assignment has been found. Its intensity, comparable to that of the 1013.6 cm^{-1} band, discards the possibility of a hot band. In the following, we will assume that both bands belong to the same vibration (ν_{23}) split by internal rotation and we proceed to the very challenging rovibrational analysis in the ν_{23} band region, considering the split states (-) and (+) separately. The weak intensities of *P* and *R* lines, the strong overlap between rotational branches of very close bands and the less accurate calculations does not enable to obtain a simulation at instrumental accuracy but some trends clearly appear. Fig.9b displays rough simulations of both *Q* branches complemented by few intense *P* and *R* lines which provide nearly similar estimates for the (-) and (+) components of ν_{23}: a strong decrease of A (ΔA~ -10 MHz) and the sum (ΔB + ΔC) close to zero correctly reproduce the *Q* branches. GS as well as v_{19}=1 and v_{23}=1 excited states rotational parameters of biphenyl are reported in Table 3.

IV. Discussion

A. Comparison of ground state molecular parameters with previous studies

Table 4 gathers the molecular parameters for the GS of naphthalene and [1,5] naphthyridine derived from different IR and UV-Vis studies. Concerning the IR studies, the accuracy of rotational and quartic CD constants has been improved in the present work thanks to the larger number of bands analyzed (6 for both PAHs compared to 3 for naphthalene[19] and 2 for [1,5] naphthyridine[31], previously) with different band types. In particular, quartic CD constants could be adjusted for the ground state of [1,5] naphthyridine while they were kept fixed to calculated values in the previous IR study. The rotational data of naphthalene derived from the electronic spectra of Yoshida *et al*[24] seem to be more accurate than ours (especially for *B* and *C*) but surprisingly, rather different values were obtained for the quartic CD constants Δ_K and Δ_{JK} with a degraded precision. We believe that the present data set, incorporating all the experimental results should provide the most reliable sets of rotational constants.

The ES molecular parameters derived from the RT cell spectra confirm that naphthalene and [1,5] naphthyridine are very rigid PAHs for which rotational structures do not require higher orders of CD terms and show weak variations of quartic CD constants between the different vibrationally excited levels.

B. Comparison between theoretical and high resolution experimental results

Our updated GS molecular parameters of naphthalene reported in Table 1 confirm that the mixing method B97-1/cc-pVTZ//ANO-DZP is more predictive than B97-1/cc-pVTZ. In the following, the former will be used as reference for any comparison with our experimental rotational data.

GS and ES calculated rotational constants are compared to experimental values for the two rigid PAHs studied (Table 5). The MAE of the differences between experimental and calculated rotational constants (δ=exp-calc) are equal to 1.05 MHz for naphthalene and to 0.58 MHz for [1,5]-naphthyridine over 21 constants. After correction of the calculated values by the GS deviation, the MAE of corrected values are reduced to about 110 and 20 kHz while in previous IR studies it was 430 kHz (9 constants for naphthalene) and 180 kHz (6 constants for [1,5] naphthyridine). Such a reduction of the corrected MAE by a factor 4 and 6, respectively, gives high confidence in the predictive power of these corrected calculated rotational constants.

In the case of biphenyl, only the ν_{19} band analysis is satisfying and we obtained a corrected MAE value close to 350 kHz, a value larger than for rigid PAHs. Quantum chemical calculations fail to correctly model the flexibility of the carbon bond bridge between two phenylic groups which tends to be sensitive to the environment (medium, temperature, etc.). Within the gas-phase experiments, Bastiansen *et al.*[48] mentioned that the dihedral angle θ has been experimentally determined to about 42° at RT to be compared with our theoretical structure optimized around 39° for which the rotational parameters are rather well predicted. This slightly different geometry might explain the higher MAE value than for rigid PAHs. As a perspective, the method/basis-set for this model could be especially optimized using parallel tempering dynamics techniques[49] to confirm their reliance between the distortion and environment influence. Last, more vibrational bands of biphenyl should be analyzed to evaluate the predictive character of the theoretical method used for this flexible PAH, but the observation of rotationally resolved IR bands of biphenyl in various spectral regions is expected to be challenging.

C. GS and ES Inertial defects

The inertial defect of a molecule is defined as $\Delta = I_{cc} - I_{aa} - I_{bb}$ where I_{xx} ($x = a, b, c$) are the principal moments of inertia of the molecule. For a planar rigid rotor, the value of the inertial defect should be zero and negative for non planar rigid molecules. For planar molecules, slightly negative values can be obtained as a balance between the negative contribution of very low-frequency oop vibrations which overcomes the positive contribution of in-plane vibrations. The negative sign of experimental inertial defect values ($\Delta_{GS,exp}$) is a consequence of the large contribution from the low-lying oop vibrations, increasing with the number of rings, confirmed by the sharp increase of $\Delta_{GS,exp}$ values from about -0.14 to -0.60 amu Å^2 from two-ring to four-ring PAHs.

From Morino's general formula for inertial defects, Oka established a simple empirical relation[50],

$$\Delta_{0exp} = \Delta_{0l} + \alpha\sqrt{I_{cc}} \qquad (1)$$

$$\Delta_{0l} = -\frac{33.715}{\nu_l} \quad (2)$$

and

where Δ_{0exp} is the experimental inertial defect, Δ_{0l} is the zero-point inertial defect, ν_l is the frequency of the lowest oop vibration, I_{cc} is the inertial moment about the *c* axis and α is a constant empirical parameter.

Oka successfully applied this formula to monocyclic aromatic molecules, assuming that the dominant effect comes from the lowest frequency oop vibration. Following the same procedure as Oka, Jahn *et al*.**Erreur ! Signet non défini.** extended its methodology to establish an empirical relation which includes a number of oop modes equal to the number of rings of the PAH, or for molecules with an extra low frequency oop vibration (< 100 cm^{-1}), equal to the number of rings +1:

$$\Delta_{0exp} = -\sum_{l=1}^{n} \frac{33.715}{\nu_l} + \alpha\sqrt{I_{cc}} \quad (3)$$

where *n* is the number of low frequency oop modes, equal or +1 larger than the number of rings.

Table 6 reports experimental inertial defects measured in the GS for a list of 20 PAHs, including 16 two-rings PAHs using data derived from MW spectroscopy ([1,6] naphthyridine[31], azulene[9], isoquinoline[51], quinoline[51], phtalazine[52], quinazoline[52], quinoxaline[52], 1- and 2-naphthaldehyde[53], 3 conformers of 1- and 2- hydroxynaphthalene[54] (due to its non-planarity, the cis-1-hydroxynaphthalene has been discarded) and updated IR data from our measurements for [1,5] naphthyridine and naphthalene as well as 3 three-ring PAHs and one four-ring PAH including corrected GS rotational constants for acenaphtylene[9], phenanthridine[55], [1,10] phenanthroline[10] and pyrene[56].

According to the fit of Jahn *et al*.**Erreur ! Signet non défini.** the vibrational frequencies of the lowest oop modes of 20 PAHs either determined from FTIR spectroscopy or DFT anharmonic calculations are included in Table 6 to test the validity of eqn (3). As evidenced by Hazrah *et al.*[54] the calculated inertial defect values of cis-2-, trans-1- and trans-2-hydroxynaphthalene for different numbers of oop vibrations highlight either a slightly overestimated value (with *n*+1 = 3 modes) or a slightly underestimated value (with *n* = 2 modes). The same tendency is observed with 1- and 2-naphthaldehyde: their calculated inertial defect rises to 0.46 and 0.49 amu $Å^2$ (about 0.15 amu $Å^2$ larger than the fit of Jahn *et al.*), respectively, when the three lowest oop modes are used to account for the presence of an extra low frequency oop vibration. Fig 10 displays a plot of the difference between measured and calculated zero point inertial defects versus the square root of the c-axis moment of inertia. A better match is obtained when considering only two oop modes: the data set of 20 PAHs is fitted to a straight line (R^2=0.90) with a slope α value of 0.010(1) to consider when using eqn (3). As already suggested by Hazrah *et al.*[54], the degree of flexibility of the hydroxyl (and the aldehyde) group in hydroxynaphthalenes (and naphthaldehydes) is probably responsible for the deviation to the Jahn *et al.* fit.

Combined fits of both naphthalene and [1,5] naphthyridine enable us to determine ES inertial defects for butterfly (ν_{48} and ν_{22}), drumhead (ν_{24}, ν_{47} and ν_{42}), oop C-H bending (ν_{46} and ν_{18}), in plane (ip) C-H bending (ν_{35} and ν_{39}) and ring C-C stretching (ν_{19} and ν_{32}) modes and to compare them with anharmonic calculations. Table 7 reports inertial defects in the GS and 6 ES for these two rigid PAH molecules. As already observed in previous studies[57,58], inertial defect values are well correlated with the amplitude of oop vibrational motions. Most negative values of Δ_{ES} are obtained for butterfly and oop C-H bending modes. More generally, Δ_{ES} values for a vibrational motion are about similar whatever the molecule. As Δ_{ES} is very sensitive to rotational constants values, the comparison experiment-theory can be useful to point out a local perturbation not taken into account in the quantum calculations, as for example a Coriolis coupling with a close vibrational mode. A good agreement between $\Delta_{ES,exp}$ and $\Delta_{ES,calc}$ is found for most of vibrational modes investigated, except for the drumhead ν_{47} mode of naphthalene, the ring C-C stretching ν_{32} mode of [1,5] naphthyridine and the CH ring ip bend of both PAHs.

Conclusion

In this study, we performed a jet-cooled high resolution mid-infrared laser spectroscopy study of naphthalene, [1,5] naphthyridine and biphenyl in both regions of in plane ring C-H bending (975-1035 cm^{-1}) and C-C ring stretching (1580-1620 cm^{-1}) vibrations. For these two-ring centrosymmetric PAHs, the complementarity between supersonic jet and RT long path cell set-ups coupled to infrared spectroscopy methods, supplemented by quantum chemistry calculations, is an efficient strategy to derive accurate ground and excited states molecular parameters from rovibrational analyses of high resolution spectra. With respect to previous studies on naphthalene and [1,5] naphthyridine, combined fits of 6 rovibrational bands have been performed, including all possible projections of the dipole moment following the molecular axis (c-type for out-of-plane vibrations, a- and b-type for in-plane vibrations). Such a large panel of vibrations gives access to different selection rules regarding the parities of ΔK_a and ΔK_c and strongly reduces the correlations between molecular parameters. The improvement in accuracy of ground state molecular data with respect to previous studies illustrates the advantages of tunable QCL-jet assemblies for the high resolution investigation of large heavy polyatomic molecules. The predictive power of anharmonic DFT calculations is largely confirmed here with a corrected MAE reduced to 110 and 20 kHz over 21 constants for naphthalene and [1,5] naphthyridine, respectively.

First jet-cooled spectra of two bands (ν_{19}, ν_{23}) of biphenyl have been recorded in the mid-IR region with the SPIRALES set-up. Due to the flexibility of its single bond between phenyl rings, very low frequency out-of-plane torsional vibrations are probably responsible for a rich internal dynamics. As a consequence, spectral congestion and unidentified features encountered in the rovibrational analysis of these bands highlight the need to use more adapted calculation methods as for example parallel tempering simulations for investigating such flexible PAHs.

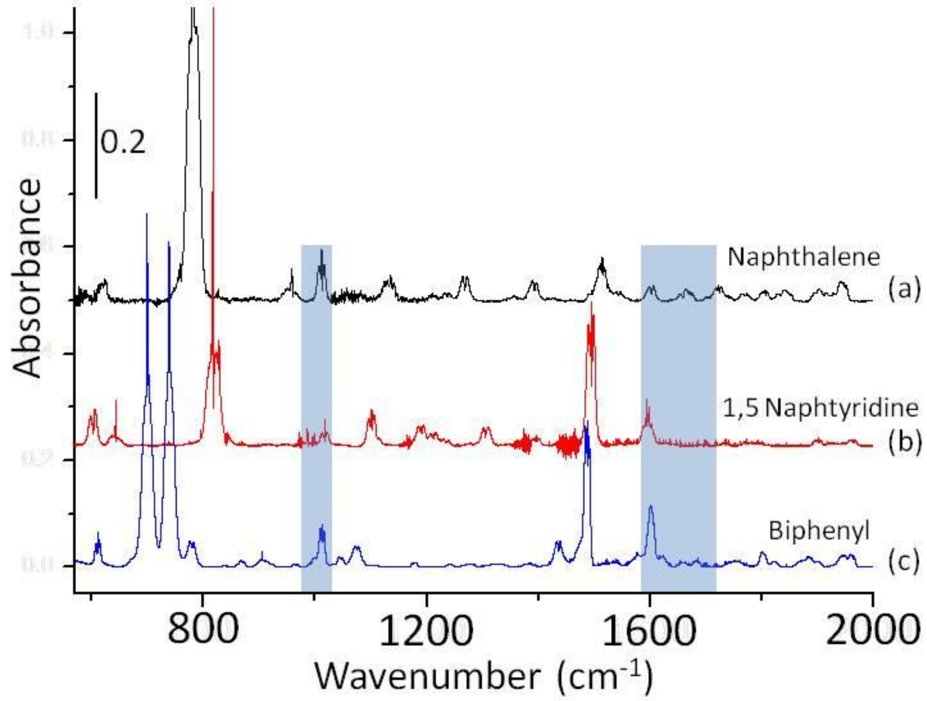

Fig 1: Fourier transform spectra of three bicyclic centrosymmetric PAHs recorded at 0.5 cm^{-1} resolution: (a) naphthalene, (b) [1,5] naphthyridine, (c) biphenyl. Only the 550-2000 cm^{-1} mid-IR range is displayed in which most of fundamental bands fall. The shaded blue regions represent the narrow spectral ranges covered by the three QCLs available at MONARIS.

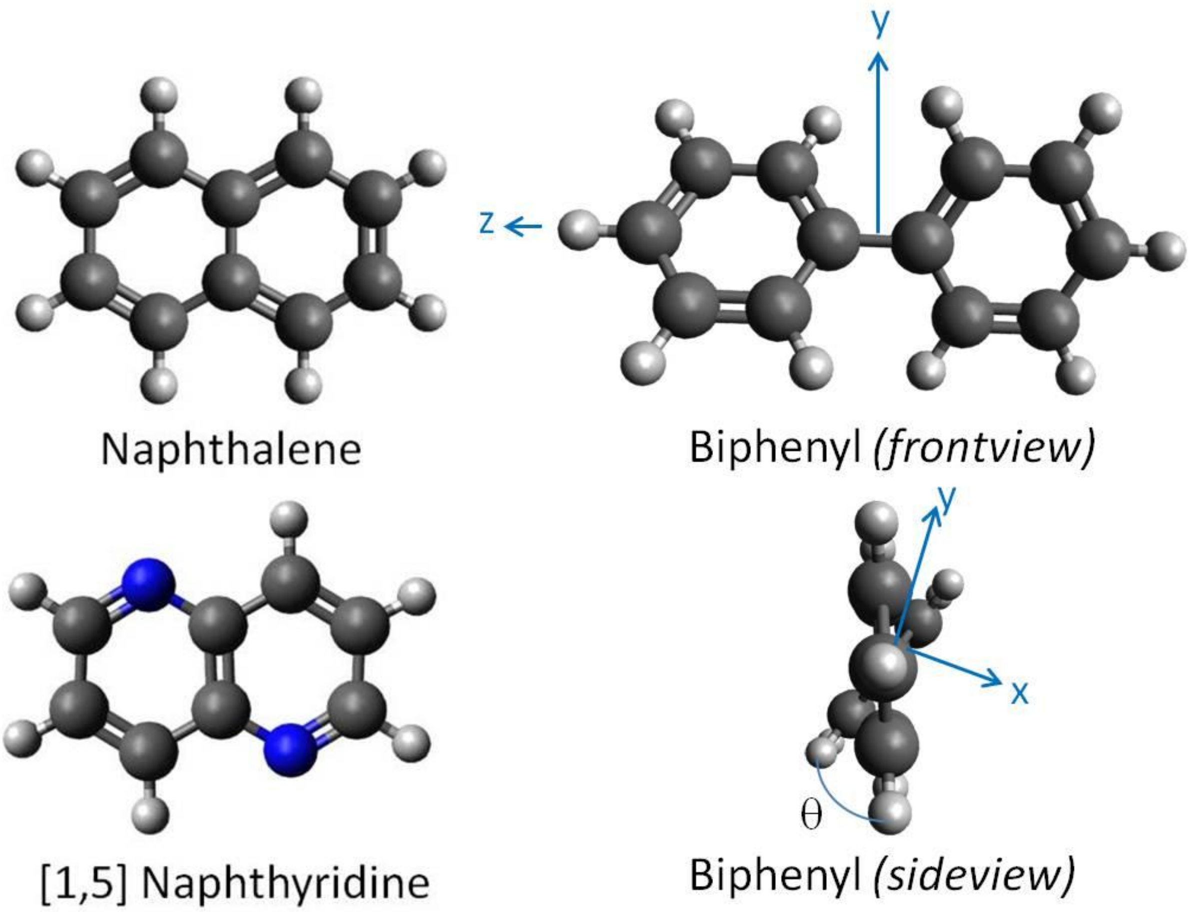

Fig. 2: Calculated equilibrium geometry (B97-1/ANO-DZP) of the three two-ring PAHs: naphthalene, [1,5] naphthyridine and biphenyl with axes definition and the dihedral angle θ.

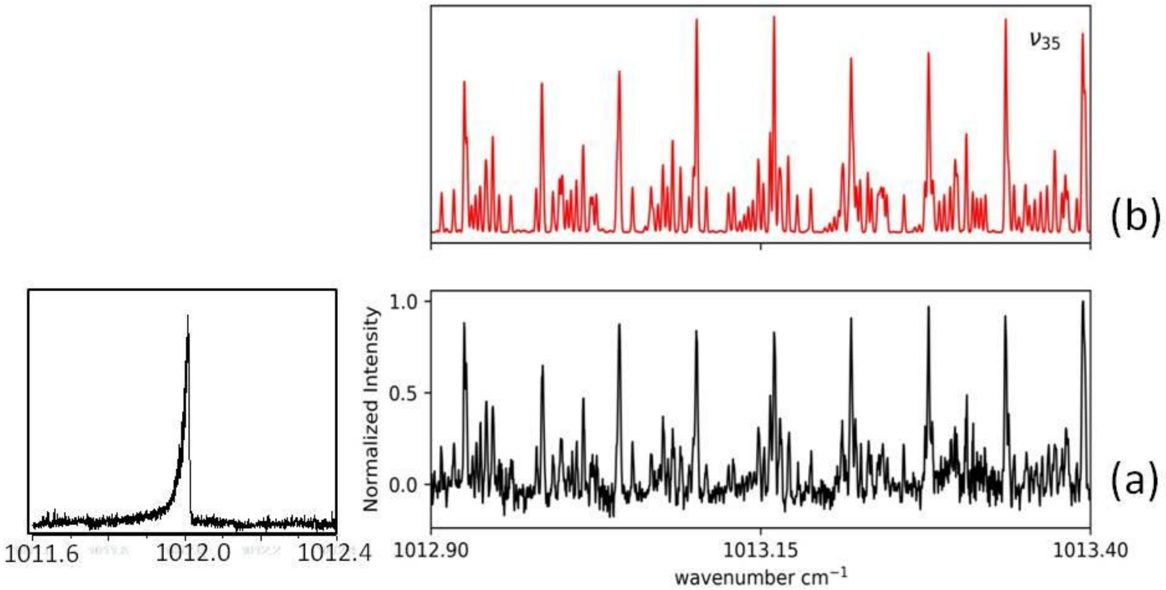

Fig. 3: Expanded view of *Q*- and *R*- branches of the ν_{35} a-type band of naphthalene. (a) The experimental jet-cooled SPIRALES spectrum, (b) the spectrum simulated at T_{rot} = 25(5) K using constants from the best fit.

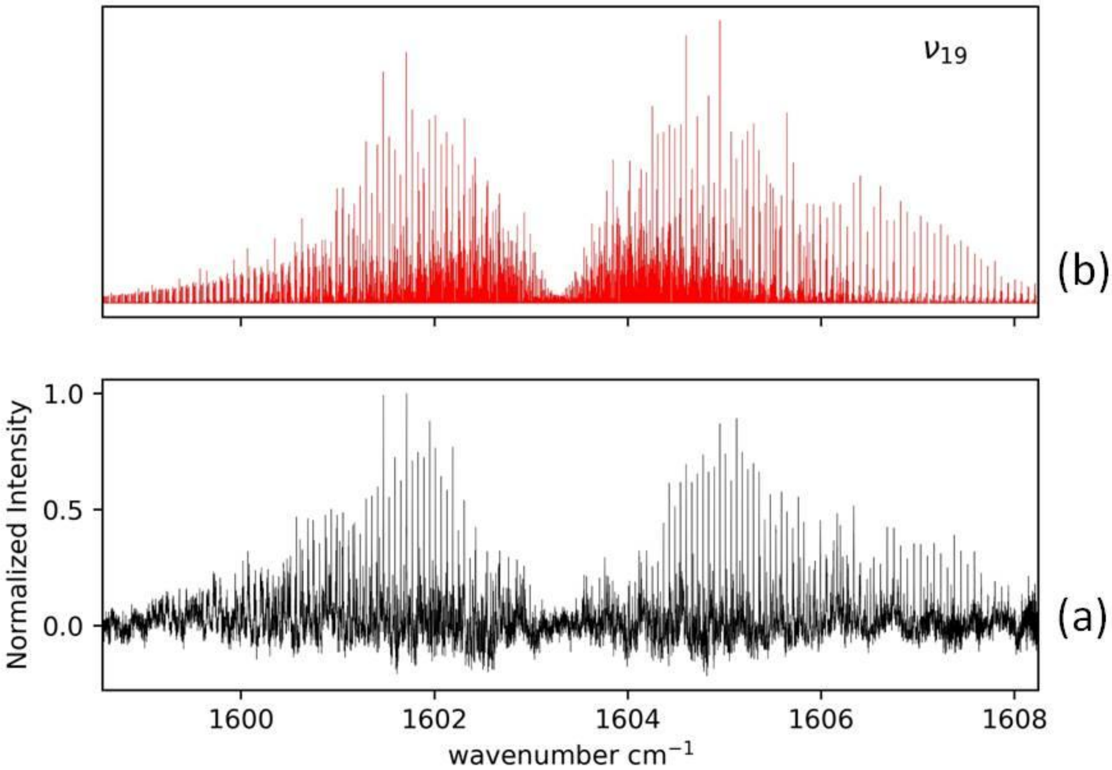

Fig. 4: Overall view of the ν_{19} b-type band of naphthalene. (a) The experimental jet-cooled SPIRALES spectrum, (b) the spectrum simulated at T_{rot} = 25(5) K using constants from the best fit.

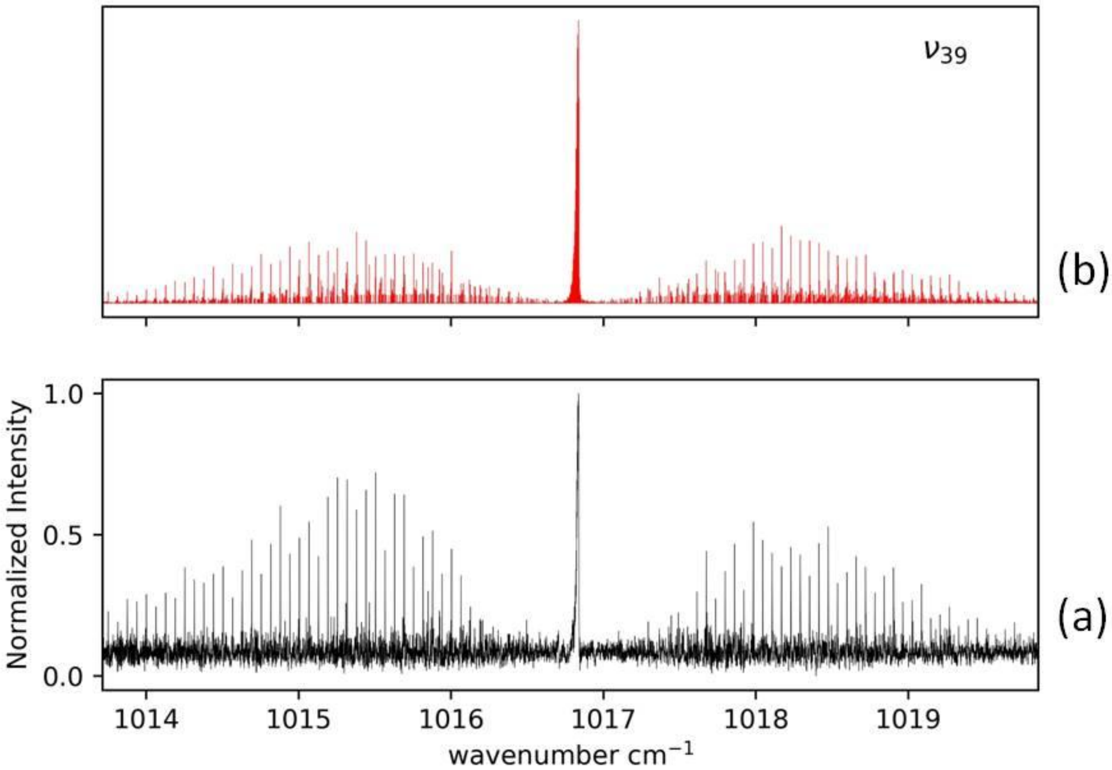

Fig. 5: Overall view of the ν_{39} band of [1,5] naphthyridine. (a) The experimental jet-cooled SPIRALES spectrum, (b) the spectrum simulated at T_{rot} = 25(5) K using constants from the best fit.

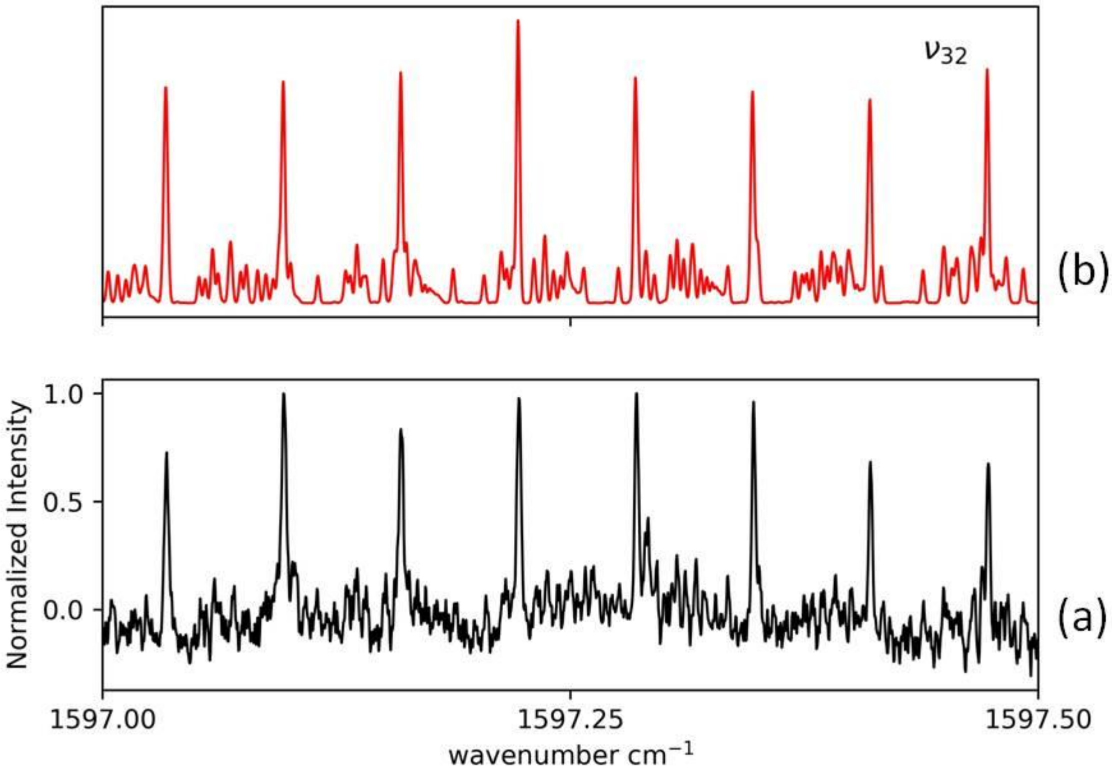

Fig. 6: Expanded view in the low *J* region of the P-branch of the ν_{32} band of [1,5] naphthyridine. (a) The experimental jet-cooled SPIRALES spectrum, (b) the spectrum simulated at T_{rot} = 25(5) K using constants from the best fit.

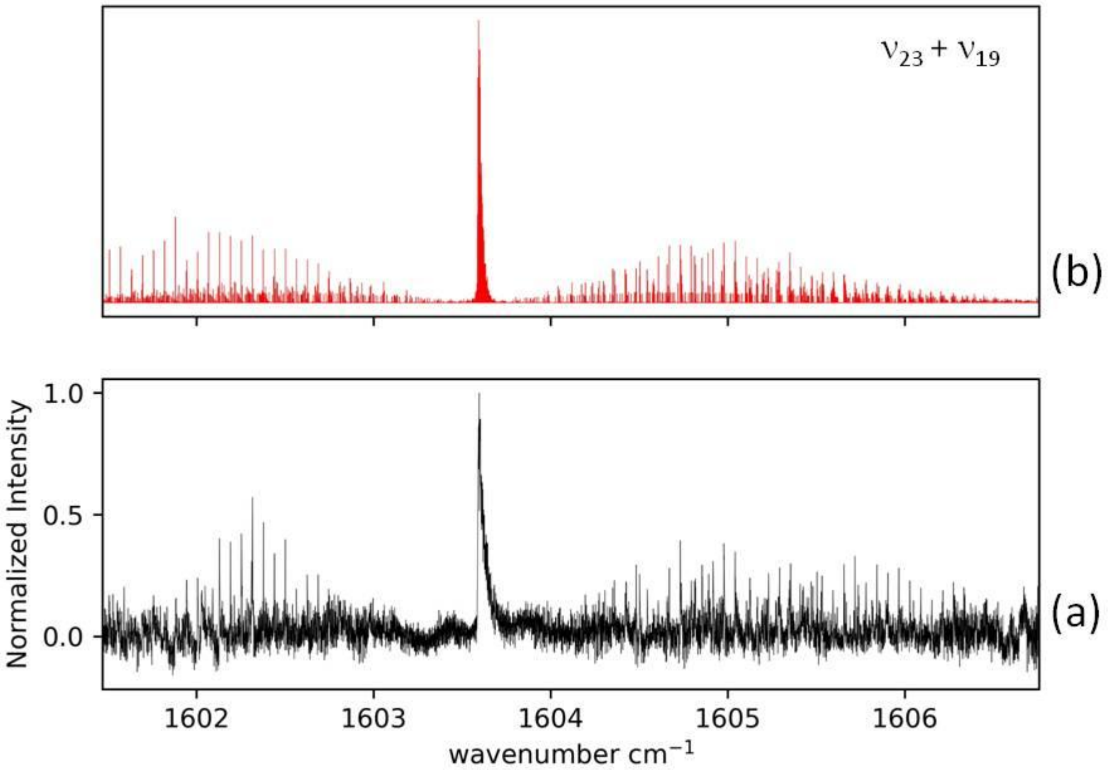

Fig. 7: Overall view of the (ν_{23}+ν_{19}) combination band of [1,5] naphthyridine. (a) The experimental jet-cooled SPIRALES spectrum, (b) the spectrum simulated at T_{rot} = 25(5) K using constants from the best fit.

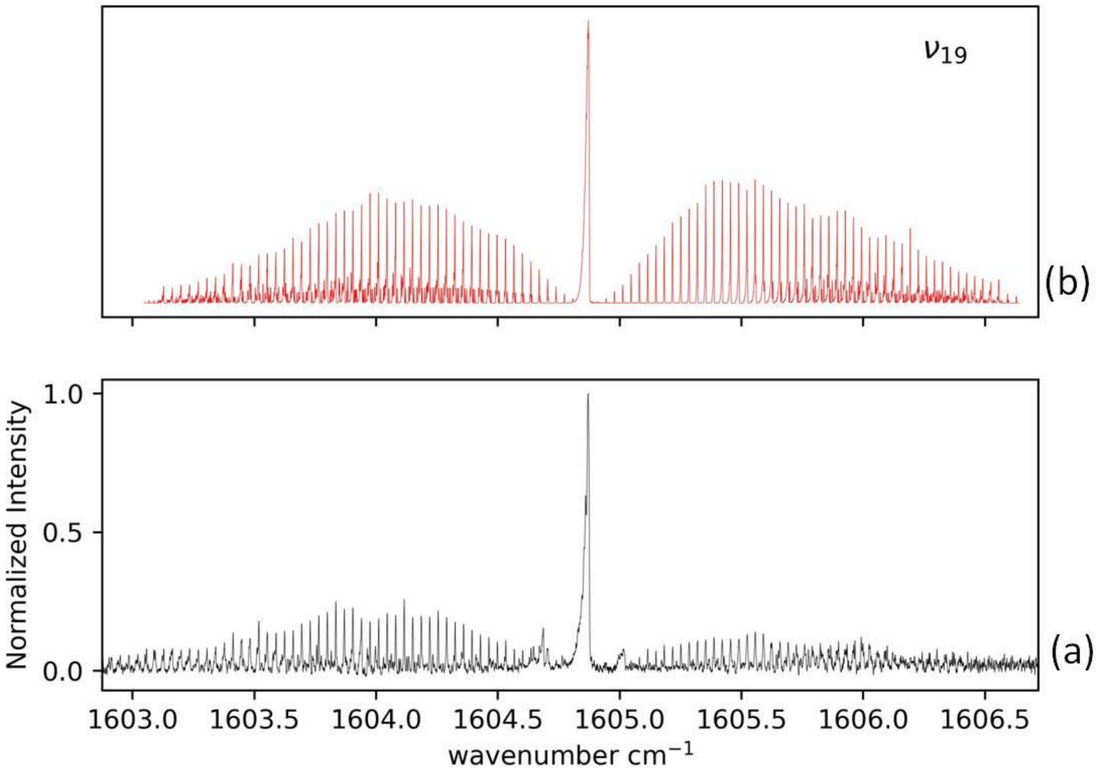

Fig. 8: Overall view of the ν_{19} band of biphenyl. (a) The experimental jet-cooled SPIRALES spectrum, (b) the spectrum simulated at $T_{rot} = 20(5)$ K. Hot band patterns are observed on the red side of the Q-branch and in the low *J* region of *P*- and *R*-branches.

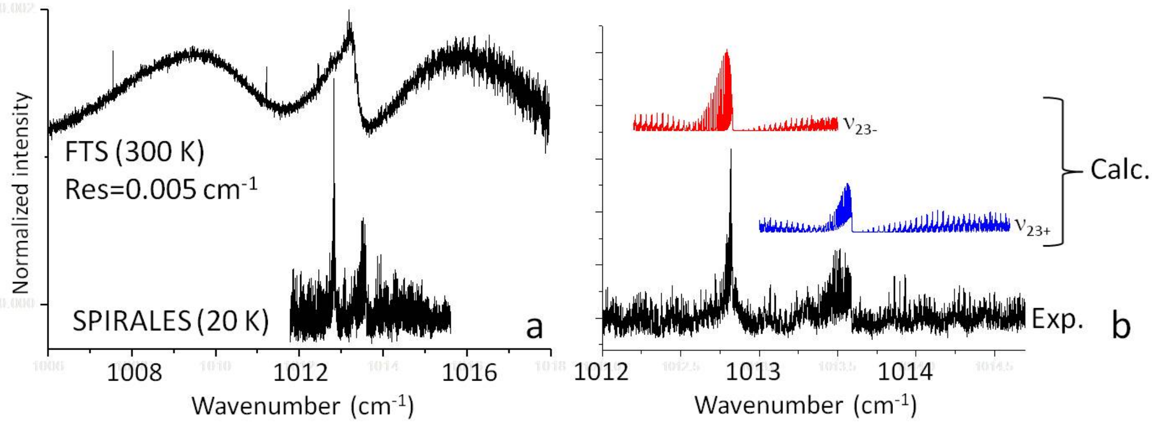

Fig. 9: a- High resolution spectrum of the ν_{23} band of biphenyl: FTS spectrum in a RT long path cell at 0.005 cm^{-1} resolution (top) and SPIRALES jet-cooled spectrum at about T_{rot}=20 K (bottom). Comparison between Q branch band contours recorded at 300 K and at low temperature clearly shows that the Q branch peaked at 1013.6 cm^{-1} in the cold spectrum corresponds to the onset of the broad Q branch observed using FTS. b- Rough simulation of both components (-) and (+) of the ν_{23} band compared to the experimental one.

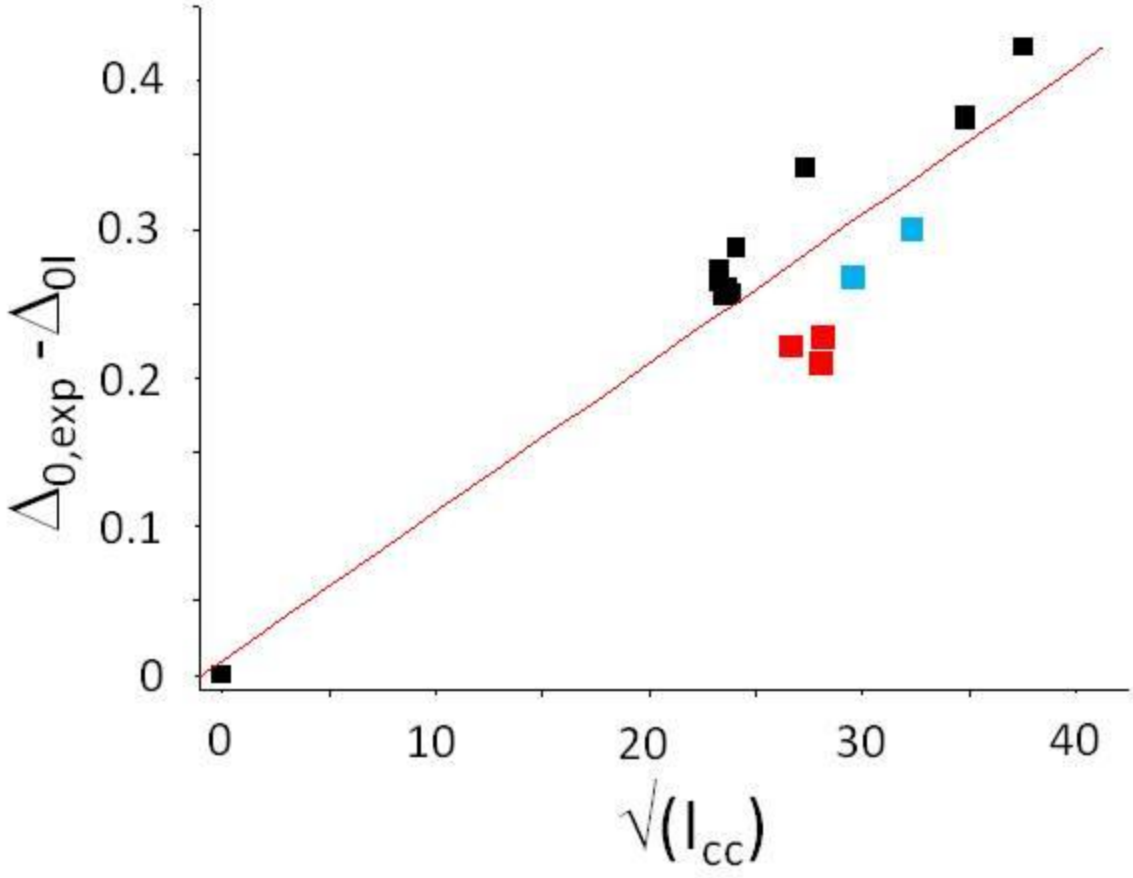

Fig.10: Plots of $\Delta_{0,exp} - \Delta_{0l}$ in amu Å^2 as a function of $\sqrt{I_{cc}}$. The points for the 20 PAHs have been determined from eqn (3) by considering only the two lowest frequency oop modes for all two-ring species, three ones for three ring species and five ones for pyrene (cf Table 6). The more "functionalised" two-ring PAHs (hydroxynaphthalenes in red and naphthaldehydes in blue) deviate toward larger inertial defect values when an extra lowest out of plane mode frequency is added according to the fit of Jahn et al.[56]

	B971/cc-pVTZ	B971/cc-pVTZ //ANO-DZP	Experimental						
Parameters	GS		GS	ν_{48}	ν_{24}	ν_{47}	ν_{46}	ν_{35}	ν_{19}
Band center (cm^{-1})				166.65843(2)	359.06177(2)	473.73950(1)	782.33081(1)	1012.01379(4)	1603.28695(5)
A	**3104.5907**	**3121.7988**	3119.3674(26)	3112.8152(28)	3124.284(35)	3119.3662(27)	3113.6492(27)	3116.564(18)	3118.786(13)
B	**1226.6308**	**1233.1063**	1232.9492(91)	1233.819(11)	1233.1865(79)	1233.465(14)	1232.859(12)	1232.974(12)	1231.826(13)
C	**879.4112**	**884.1779**	883.8819(45)	884.740(10)	883.6822(45)	883.490(15)	883.802(11)	883.581(5)	883.4787(50)
$\Delta_J(x10^3)$	**0.0178**	**0.0178**	0.0180 (4)	0.0171(4)	0.0182(4)	0.0228(5)	0.0208(4)	0.0180[b]	0.0180[b]
$\Delta_K(x10^3)$	**0.149**	**0.149**	0.175(1)	0.155(1)	0.530(47)	0.184(1)	0.133(1)	0.175[b]	0.175[b]
$\Delta_{JK}(x10^3)$	**0.0459**	**0.0459**	0.0246(13)	0.0386(15)	0.002(3)	0.0104(13)	0.0204(13)	0.0246[b]	0.0246[b]
$\delta_J(x10^6)$	**5.25**	**5.25**	5.25[a]	5.25[a]	5.25[a]	5.25[a]	5.25[a]	5.25[a]	5.25[a]
$\delta_K(x10^6)$	**58.5**	**58.5**	58.5[a]	58.5[a]	58.5[a]	58.5[a]	58.5[a]	58.5[a]	58.5[a]
IR RMS				0.0002	0.00029	0.0002	0.00022	0.00032	0.00053
N lines				3924	1591	5142	5043	948	929
J''				14-86	5-98	14-90	7-80	2-50	3-46
K_a''				14-60	0-9	14-65	0-69	0-17	0-24

[a] δ_J and δ_K values fixed to the DFT value for all simulations

[b] fixed to the GS experimental value.

Table 1: Molecular parameters (in MHz) of the ground state, v_{46}=1, v_{47}=1, v_{48}=1, v_{24}=1, v_{35}=1 and v_{19}=1 states of naphthalene derived from a global fit of seven states. The set of experimental ground state parameters is compared to calculated ones from two different combinations of method/basis set.

Parameters	**B971/cc-pVTZ //ANO-DZP GS**	Experimental						
		GS	ν_{22}	ν_{42}	ν_{18}	ν_{39}	ν_{32}	$\nu_{23}+\nu_{19}$
Band center (cm^{-1})	**3173.3332**		166.23883(1)	395.20442(2)	817.83652(2)	1016.84235(3)	1598.68667(3)	1603.58769(5)
A	**1309.2836**	3170.9621(45)	3168.8048(46)	3175.8556(111)	3166.2623(46)	3168.4336(114)	3171.9511(129)	3174.5434(144)
B	**927.0782**	1312.1169(65)	1312.0150(71)	1312.1839(65)	1311.8106(67)	1311.9533(80)	1311.2675(85)	1311.8109(101)
C	**0.01946**	928.2951(35)	929.0125(56)	928.0521(37)	928.3125(40)	927.9606(37)	927.7712(40)	928.1528(51)
$\Delta_J(x10^3)$		0.0205(3)	0.0208(3)	0.0206(3)	0.0232(3)	0.0205[b]	0.0205[b]	0.0205[b]
$\Delta_K(x10^3)$	**0.1724**	0.1718(16)	0.1789(18)	0.1936(90)	0.1573(17)	0.1718[b]	0.1718[b]	0.1718[b]
$\Delta_{JK}(x10^3)$	**0.0480**	0.0466(11)	0.0484(12)	0.0433(15)	0.0444(11)	0.0466[b]	0.0466[b]	0.0466[b]
$\delta_J(x10^6)$	**5.86**	5.86[a]	5.86[a]	5.86[a]	5.86[a]	5.86[a]	5.86[a]	5.86[a]
$\delta_K(x10^6)$	**61.3**	61.3[a]	61.3[a]	61.3[a]	61.3[a]	61.3[a]	61.3[a]	61.3[a]
IR RMS			0.00015	0.00022	0.0002	0.00031	0.0005	0.00052
N lines			2469	1138	1955	931	678	408
J''			9-100	13-100	11-91	4-49	0-47	5-37
K_a''			9-51	0-37	9-51	0-22	0-20	0-22

[a] δ_J and δ_K values fixed to the DFT value for all simulations

[b] fixed to the GS experimental value.

Table 2: Molecular parameters (in MHz) of the ground state, v_{22}=1, v_{18}=1,v_{42}=1, v_{39}=1, v_{32}=1 and v_{23},v_{19}=1,1 states of [1,5] naphthyridine derived from a combined fit of seven states. The set of experimental ground state parameters is compared to the calculated ones from B97-1/cc-pVTZ//ANO-DZP.

Parameters	**B971/cc-pVTZ //ANO-DZP GS**	Experimental GS	ν_{19}	ν_{23-}	ν_{23+}
Band center (cm^{-1})			1604.87691(4)	1012.8304(1)	1013.5922(1)
A	**2845.9598**	2845.9598[a]	2844.87(2)		
ΔA				-10.4	-10.3
B	**529.4035**	527.453(43)	525.58(5)		
ΔB				+2.09	-1.58
C	**499.4542**	500.106(44)	501.33(5)		
ΔC				-2.09	+1.14
Δ_J(x10^3)	**0.02327**				
Δ_K(x10^3)	**0.1573**				
Δ_{JK}(x10^3)	**-0.0077**				
δ_J(x10^6)	**-2.99**				
δ_K(x10^6)	**1174**				
IR RMS			0.0004	0.0007	0.007
N lines			705	130	130
J''			3-57	3-19	3-20
K_a''			0-14	0-15	0-17

[a]Fixed to the GS DFT value.

Table 3: Molecular parameters (in MHz) of the GS, v_{19}=1 and v_{23}=1 states of biphenyl. Excited state quartic centrifugal distortion constants have been fixed to ground state values.

	Naphthalene			[1,5] Naphthyridine	
Parameters	This work	Pirali *et al.*[19]	Yoshida *et al.*[24]	This work	Gruet *et al.*[31]
A	3119.3674(26)	3119.3956(38)	3119.4026(48)	3170.9621(45)	3170.9675(20)
B	1232.9492(91)	1232.9663(111)	1232.9532(8)	1312.1169(65)	1312.0922(45)
C	883.8819(45)	883.8947(41)	883.9023(2)	928.2951(35)	928.2887(37)
Δ_J(x10^3)	0.0180 (4)	0.0158(15)	0.0174(6)	0.0205(3)	0.019462[a]
Δ_K(x10^3)	0.175(1)	0.169(4)	0.0561(96)	0.1718(16)	0.172396[a]
Δ_{JK}(x10^3)	0.0246(13)	0.0361(44)	0.0354(66)	0.0466(11)	0.047954[a]

[a]Fixed to the DFT value

Table 4: Molecular parameters (in MHz) for the naphthalene and [1,5] naphthyridine ground states obtained from the present work and previous IR and UV-Vis studies.

		Naphthalene			
		Calculated	Experimental	δ=exp-calc	ES constants corrected from GS deviation[a]
GS	A	3121.7988	3119.3674	-2.431	
	B	1233.1063	1232.9492	-0.157	
	C	884.1779	883.8819	-0.296	
ν_{48}	A	3115.0535	3112.8152	-2.238	0.193
	B	1234.0957	1233.819	-0.277	-0.12
	C	885.0773	884.740	-0.337	-0.041
ν_{24}	A	3127.3150	3124.284	-3.031	-0.6
	B	1233.3162	1233.1865	-0.13	0.027
	C	883.9980	883.6822	-0.316	-0.02
ν_{47}	A	3121.8588	3119.3662	-2.493	-0.062
	B	1233.0464	1233.465	0.419	0.576
	C	884.5077	883.490	-1.018	-0.722
ν_{46}	A	3117.7516	3113.6492	-4.102	-1.671
	B	1232.9564	1232.859	-0.097	0.06
	C	884.2379	883.802	-0.436	-0.14
ν_{35}	A	3119.6103	3116.564	-3.046	-0.615
	B	1233.1363	1232.974	-0.162	-0.005
	C	883.8481	883.581	-0.267	0.029
ν_{19}	A	3120.2399	3118.786	-1.454	0.977
	B	1231.9371	1231.826	-0.111	0.046
	C	883.6083	883.4787	-0.13	0.16
		[1,5] naphthyridine			
GS	A	3173.3332	3170.9621	-2.371	
	B	1309.2836	1312.1169	2.833	
	C	927.0782	928.2951	1.217	
ν_{22}	A	3171.6243	3168.8048	-2.820	-0.449
	B	1309.1337	1312.0150	2.881	0.048
	C	927.7977	929.0125	1.215	-0.002

ν_{42}	A	3178.2797	3175.8556	-2.424	-0.053
	B	1309.4035	1312.1839	2.880	0.047
	C	926.8683	928.0521	1.184	-0.033
ν_{18}	A	3169.2260	3166.2623	-2.964	-0.593
	B	1309.0438	1311.8106	2.767	-0.066
	C	927.1382	928.3125	1.174	-0.043
ν_{39}	A	3171.2946	3168.4336	-2.861	-0.490
	B	1309.2536	1311.9533	2.700	-0.133
	C	926.7484	927.9606	1.212	-0.005
ν_{32}	A	3171.3545	3171.9511	0.597	2.968
	B	1308.0245	1311.2675	3.243	0.410
	C	926.4486	927.7712	1.323	0.106
$\nu_{23}+\nu_{19}$	A	3178.4896	3174.5434	-3.946	-1.575
	B	1308.5041	1311.8109	3.307	0.474
	C	927.1981	928.1528	0.955	-0.262
			Biphenyl		
GS	A	2845.9598	2845.9598[c]	-	
	B	529.4035	527.453	-1.950	
	C	499.4542	500.106	0.652	
ν_{19}	A	2843.412	2844.868	1.456	1.458
	B	528.654	525.580	-3.074	-1.124
	C	499.964	501.331	1.367	0.715

[a]Corrected values correspond to calculated ES constants corrected by the GS deviation.
[b]Experimental GS rotational constant fixed to the calculated GS values.
[c]Experimental ES rotational constant fixed to the experimental GS values (see text).

Table 5: Deviations (exp – calc) on the rotational constants in the ground and excited states of naphthalene, [1,5]-naphthyridine and biphenyl. All the values are in MHz.

	$\sqrt{I_{cc}}$	$\Delta_{GS,exp}$	Lowest oop modes ν_l					Number of rings	$\Delta_{0exp} + \sum_{l=1}^{n} \frac{33.715}{\nu_l}$
[1,6] naphthyridine	23.5042	-0.1311	166.99[a]	177.81[a]	-	-		2	0.2606
Azulene	24.0918	-0.1552	142.99[a]	163[b]	-	-		2	0.2876
Isoquinoline	23.7927	-0.1336	166[b]	181[b]	-	-		2	0.2559
Phtalazine	23.7397	-0.1414	166[c]*	170[c]*	-	-		2	0.2601
Quinazoline	23.5017	-0.1407	158.09[a]	174.7[d]	-	-		2	0.2552
Quinoline	23.6216	-0.1322	168[b]	178[b]*	-	-		2	0.2580
Quinoxaline	23.3319	-0.1357	154.36[a]	177.01[d]	-	-		2	0.2732
[1,5] naphthyridine	23.3327	-0.1240	166.24[a]	181.39[a]	-	-		2	0.2648
Naphthalene	23.9118	-0.1356	166.66[a]	178[e]*	-	-		2	0.2562
Trans-1-hydroxynaphthalene	26.5673	-0.2124	141[f]*	173[f]*				2	0.2217
Cis-2-hydroxynaphthalene	28.1069	-0.2365	122[f]*	182[f]*				2	0.2252
Trans-2-hydroxynaphthalene	28.0989	-0.251	122[f]*	181[f]*				2	0.2106
1-naphthaldehyde	29.5044	-0.4129	76[g]	143[g]				2	0.2666
2-naphthaldehyde	32.3907	-0.3663	75[g]*	152[g]				2	0.3051
Acenaphthylene	27.3518	-0.1924	155[h]	206[h]*	222[h]*	-		3	0.3408
Phenanthridine	34.8334	-0.4577	96[i]*	101[i]*	227[i]*	-		3	0.3759
Phenanthroline	34.8334	-0.4423	100[j]*	103[j]*	223[j]*	-		3	0.3734
Pyrene	37.521	-0.5828	98[k]*	150*	209*	240*	254*	4	0.4226

[a]Ref.[31]. [b]Ref.[59] [c]B3LYP/6-31G (Ref. [60]) [d]Ref. [61]. [e]B3LYP/Def2TZVPP]. [f]Ref.[54]. [g]Ref.[53]. [h]B3LYP/Def2TZVPP.
*[i]B3LYP/6-311G** (Ref.[55]). [j]BP86/RI/TZVP (Ref.[62]) [k]Ref.[63]. The calculated frequencies of lowest oop modes are denoted (*).*

Table 6: Ground state experimental inertial defects (amu Å^2). and lowest frequency oop modes (cm^{-1}) used to derive the empirical parameters.

		GS	Butterfly mode	Drumhead modes		CH oop bend	CH ring ip bend	CC ring stretch
Naphthalene	Exp.	-0.136	-0.742	0.327	0.289	-0.411	0.078	-0.279
	Calc.	*-0.149*	*-0.751*	*0.323*	*-0.379*	*-0.447*	*-0.039*	*-0.250*
[1,5] naphthyridine	Exp.	-0.124	-0.683	0.284		-0.461	-0.103	-0.016
	Calc.	*-0.124*	*-0.677*	*0.283*		*-0.463*	*-0.041*	*-0.224*

Table 7: Comparison between ground and excited states inertial defects (amu Å^2) of naphthalene and [1,5] naphthyridine derived from rovibrational analyses (Exp.) and anharmonic quantum calculations (Calc.)

References

[1]A. Léger and J. L. Puget, Astron. Astrophys. **137**, L5 (1984).

[2]A. G. G.M. Tielens, Annu. Rev. Astron. Astrophys. **46**, 289 (2008).

[3]C. Jäger, F. Huisken, H. Mutschke, I. Llamas Jansa and Th. Henning , **696**, 706 (2009).

[4]B.A. Mc Guire, A. M. Burkhardt, C. N. Shingledecker, A. J. Remijan, E. Herbst and M. C. Mc Carthy, Science, **359**, 202 (2017).

[5]B.A. Mc Guire, R.A. Loomis, A. M. Burkhardt, K.L. K. Lee, C. N. Shingledecker, S. B. Charnley, I. R. Cooke, M. A. Cordiner, E. Herbst, S. Kalenskii, M. A. Siebert, E. R. Willis, C. Xue, A. J. Remijan, and M. C. Mc Carthy, Science, **371**, 1265 (2021).

[6]J. Cernicharo, M. Agundez, C. Cabezas, B. Tercero, N. Marcelino, J. R. Pardo and P. de Vicente, Astron. Astrophys. Lett. **649**, L15 (2021).

[7]O. Berne, C. Joblin, A. Fuente and F. Menard, Astron. Astrophys. **495**, 827 (2009).

[8]T. J. Balle and W.H. Flygare, Rev. Sci. Instrum. **52** 33 (1981).

[9]S. Thorwirth, P. Theule, C. A. Gottlieb, M. C. McCarthy, and P. Thaddeus, Astrophys. J. **662**, 1309 (2007).

[10] D. Mc Naughton, P. D. Godfrey, R. D. Brown, S. Thorwirth and J.-U Grabow, Astrophys. J. **678**, 309 (2008).

[11]S. Gruet, A. L. Steber and M. Schnell, J. Mol. Spectr. **371**, 111296 (2020).

[12]M. Goubet and O. Pirali, J. Chem. Phys. **140**, 044322 (2014).

[13]S. Albert, K. K. Albert, P. Lerch and M. Quack, Faraday Discuss, **150**, 71 (2011).

[14] O. Pirali, M. Vervloet, G. Mulas, G. Malloci and C. Joblin, Phys. Chem. Chem. Phys. **11**, 3443 (2009).

[15] O. Pirali, N.-T. Van-Oanh, P. Parneix, M. Vervloet and P. Brechignac, Phys. Chem. Chem. Phys. **8**, 3707 (2006).

[16] K. Zhang, B. Guo, P. Colarusso and P. F. Bernath, Science, **274**, 582 (1996).

[17]M. Herman, R. Georges, M. Hepp and D. Hurtmans, Int . Rev. Phys. Chem. **19**, 277 (2000).

[18]B. E. Brumfield, J. T. Stewart and B. J. McCall, J. Phys. Chem. Lett **3**, 1985 (2012).

[19]O. Pirali, M. Goubet, T. Huet, R. Georges, P. Soulard, P. Asselin, J. Courbe, P. Roy and M. Vervloet, Phys. Chem. Chem. Phys. **15**, 10141 (2013).

[20]M. Cirtog, P. Asselin, P. Soulard, B. Tremblay, B. Madebène and M. E. Alikhani, R. Georges, A. Moudens, M. Goubet, T.R. Huet, O. Pirali et P. Roy, J. Phys. Chem. A, **115**, 2523 (2011).

[21]B. Spaun, P. B. Changala, D. Patterson, B.J. Björk, O. H. Heckl, J. M. Doyle and J. Ye, Nature, **533** 517 (2016).

[22]P. B. Changala, M. Weichman, K.F. Lee, M. E. Fermann and J. Ye, Science **363** 49 (2019).

[23] D. L. Joo, R. Takahashi, J. O'Reilly, H. Kat and M. Baba, J. Mol. Spectrosc., **215**, 155 (2002).

[24] K. Yoshida, Y. Semba, S. Kasahara, T. Yamanaka and M. Baba, J. Chem. Phys., **130**, 194304 (2009)..

[25] P. Asselin, A. Potapov, A. C. Turner, V. Boudon, L. Bruel, M-A. Gaveau, M. Mons, Phys. Chem. Chem. Phys. **19**, 17224 (2017).

[26] P. Asselin, J. Bruckhuisen, A. Roucou, M. Goubet, M-A. Martin-Drumel, A. Jabri, Y. Belkhodja, P. Soulard, R. Georges, A. Cuisset, J. Chem. Phys. **151**, 194302 (2019) .

[27]E. Cané, A. Miani and A. Trombetti, J. Phys. Chem. A **111** 8218 (2007).

[28]V. Kasalova, W. D. Allen, H. F. Schaefer III, E. Czinki and A. G. Csaszar, J. Comput. Chem. **28** 1373 (2007).

[29]V. Barone, M. Biczysko and C. Puzzarini, Acc. Chem. Res. **48** 1413 (2015).

[30]C. Puzzarini, J. Bloino, N. Tasinato and V. Barone, Chem. Rev. **119** 8131 (2019).

[31] S. Gruet, M. Goubet and O. Pirali, J. Chem. Phys. **140**, 234308 (2014).

[32] M. A. Martin-Drumel, O. Pirali, C. Falvo, P. Parneix, A. Gamboa, F. Calvo and P. Brechignac, Phys. Chem. Chem. Phys. **16**, 22062 (2014).

[33]A. Jabri, Y. Belkhodja, Y. Berger, I. Kleiner, and P. Asselin, J. Mol. Spectrosc. **349**, 32 (2018).

[34] I.E. Gordon, L.S. Rothman, C. Hill, R.V. Kochanov, Y. Tan, P.F. Bernath, M. Birk, V. Boudon, A. Campargue, K.V. Chance, B.J. Drouin, J.-M. Flaud, R.R. Gamache, J.T. Hodges, D. Jacquemart, V.I. Perevalov A. Perrin, K.P. Shine, M.-A.H. Smith, J. Tennyson, G.C. Toon, H. Tran, V.G. Tyuterev, A. Barbe, A.G. Császár, V.M. Devi, T. Furtenbacher, J.J. Harrison, J.-M. Hartmann, A. Jolly, T.J. Johnson, T. Karman, I. Kleiner, A.A. Kyuberis, J. Loos, O.M. Lyulin, S.T. Massie, S.N. Mikhailenko, N. Moazzen-Ahmadi, H.S.P. Müller, O.V. Naumenko, A.V. Nikitin, O.L. Polyansky, M. Rey, M. Rotger, S.W. Sharpe, K. Sung, E. Starikova, S.A. Tashkun, J. Vander Auwera, G. Wagner, J. Wilzewski, P. Wcisło, S. Yu, E.J. Zak, JQSRT **203**, 3 (2017).

[35] Y. Belkhodja, J. Loreau, A. van der Avoird, Y. Berger, P. Asselin, Phys. Chem. Chem. Phys. **23** 10864 (2021).

[36]M. D. Brookes, C. Xia, J. A. Anstey, B. G. Fulsom, K.-X. Au Yong, J. M. King and A. R. W. McKellar, Spectrochim. Acta, Part A, **60**, 3235 (2004).

[37] Gaussian 09, Revision C.01, M. J. Frisch, G. W. Trucks, H. B. Schlegel, G. E. Scuseria, M. A. Robb, J. R. Cheeseman, G. Scalmani, V. Barone, G. A. Petersson, H. Nakatsuji, X. Li, M. Caricato, A. V. Marenich, J. Bloino, B. G. Janesko, R. Gomperts, B. Mennucci, H. P. Hratchian, J. V. Ortiz, A. F. Izmaylov, J. L. Sonnenberg, D. Williams-Young, F. Ding, F. Lipparini, F. Egidi, J. Goings, B. Peng, A. Petrone, T. Henderson, D. Ranasinghe, V. G. Zakrzewski, J. Gao, N. Rega, G. Zheng, W. Liang, M. Hada, M. Ehara, K. Toyota, R. Fukuda, J. Hasegawa, M. Ishida, T. Nakajima, Y. Honda, O. Kitao, H. Nakai, T. Vreven, K. Throssell, J. A. Montgomery, Jr., J. E. Peralta, F. Ogliaro, M. J. Bearpark, J. J. Heyd, E. N. Brothers, K. N. Kudin, V. N. Staroverov, T. A. Keith, R. Kobayashi, J. Normand, K. Raghavachari, A. P. Rendell, J. C. Burant, S. S. Iyengar, J. Tomasi, M. Cossi, J. M. Millam, M. Klene, C. Adamo, R. Cammi, J. W. Ochterski, R. L. Martin, K. Morokuma, O. Farkas, J. B. Foresman, and D. J. Fox, Gaussian, Inc., Wallingford CT, 2010.

[38]O. Roos, R. Lindh, P.-A. Malmqvist, V. Veryazov and P.-O. Widmark, J. Phys. Chem. A, **108**, 2851 (2005).

[39] A. D. Boese and J.M L. Martin, J. Chem. Phys. **119** 3005 (2003).

[40] H. Kruse, L. Goerigk and S. Grimme, J. Org. Chem. **77** 10824 (2012).

[41] J. K. G. Watson, in Vibration Spectra and Structure, ed.J. Durig, Elsevier, Amsterdam, **vol. 6**, .1 (1977).

[42]C. M. Western, Pgopher: JQSRT **186**, 221 (2017).

[43]H. M. Pickett, J. Mol. Spectrosc. **148**, 371 (1991).

[44]G. Zerbi and S. Sandroni, Spectrochim. Acta, Part A, , **24**, 483 (1968).

[45]O. Bastiansen, Acta Chem. Scand. **3**, 408 (1949).

[46]Y. Takei, T. Yamaguchi, Y. Osamura, K. Fuke and K. Kaya, J. Phys. Chem. **92**, 577 (1988).

[47]J. Ciolowski and S. T. Mixon, J. Am. Chem. Soc. **114**, 4382 (1992).

[48]O. Bastiansen and S. Samdal, J. Mol. Struct. **128**, 115 (1985).

[49]D. J. Earl and M. W. Deem, PCCP, **7**, 3910 (2005).

[50]T. Oka, J. Mol. Struct, **399**, 225 (1995).

[51]Z. Kisiel, O. Desyatnyk, L. Pszczolkowski, S. B. Charnley, and P. Ehrenfreund, J. Mol. Spectrosc. **217**, 115 (2003).

[52]D. Mc Naughton, P. D. Godfrey, M. K. Jahn, D. A. Dewald and J.-U Grabow, J. Chem. Phys. **134**, 154305 (2011).

[53]M. Goubet, M-A. Martin-Drumel, F. Réal, V. Vallet and O. Pirali, J. Phys. Chem. A **124** 4484 (2020).

[54]A. S. Hazrah, S. Nanayakkara, N. A. Seifert, E. Kraka and W.Jäger, PCCP, **24**, 3722 (2022).

[55]D. Mc Naughton, P. D. Godfrey, R. D. Brown and S. Thorwirth, PCCP, **9**, 591 (2007).

[56]M. K. Jahn, J.-U Grabow, M. J. Travers, D. Wachsmuth, P. D. Godfrey and D. Mc Naughton, PCCP, **19**, 8970 (2017);

[57]P. Asselin, P. Soulard, B. Madebène, M. Goubet, T. R. Huet, R. Georges, O. Pirali and P. Roy, , PCCP, **16**, 4797 (2014).

[58]S. Gruet, O. Pirali, M. Goubet, D. W. Tokaryk and P. Brechignac, J. Phys. Chem. A **120**, 95 (2016).

[59]M. A. Martin-Drumel, O. Pirali, Y. Loquais, C. Falvo and P. Brechignac, Chem. Phys. Lett. **557** 53 (2013).

[60]M. Kurt and S. Yurdakul, J. Mol. Struct. **717**, 171 (2008).
[61]S. Gruet, Thesis, University Paris-Saclay, Orsay, France (2015).
[62]M. Reiher,G. Brehm and S. Schneider, J. Phys. Chem. A **108** 734 (2004).
[63]S. Chakraborty, G. Mulas, M. Rapacioli and C. Joblin, J. Mol. Spectr. **378**, 111466 (2021)